International Journal of Pharmaceutics 636 (2023) 122808

Contents lists available at ScienceDirect

International Journal of Pharmaceutics

journal homepage: www.elsevier.com/locate/ijpharm

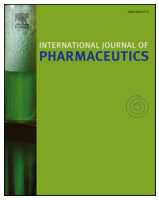

Monitoring dexamethasone skin biodistribution with ex vivo MALDI-TOF mass spectrometry imaging and confocal Raman microscopy

Eloy Pena-Rodríguez [a,1,*], Teresa García-Berrocoso [b,f,2], Ezequiel Vázquez Fernández [c,2], Francisco J. Otero-Espinar [c,d,e,3,*], Joaquin Abian [b,f,3], Francisco Fernández-Campos [a]

[a] Laboratory Reig Jofre, R&D Department, 08970, Sant Joan Despí, Barcelona, Spain
[b] Biological and Environmental Proteomics, Institut d'Investigacions Biomèdiques de Barcelona, Consejo Superior de Investigaciones Científicas (IIBB-CSIC), Institut d'Investigacions Biomèdiques August Pi i Sunyer (IDIBAPS), Barcelona, Spain
[c] Pharmacology, Pharmacy and Pharmaceutical Technology Department, Faculty of Pharmacy, University of Santiago de Compostela (USC), Santiago de Compostela, Spain
[d] Parqueasil Group, Health Research Institute of Santiago de Compostela (FIDIS), Santiago de Compostela, Spain
[e] Institute of Materials (iMATUS), University of Santiago de Compostela (USC), Santiago de Compostela, Spain
[f] Laboratorio de Proteómica CSIC/Universitat Autònoma de Barcelona (UAB), IIBB-CSIC, Barcelona, Spain

ARTICLE INFO

Keywords:
MALDI-MSI
Confocal Raman
Skin
Nanoparticle
Semiquantitative
Biodistribution

ABSTRACT

Two of the most promising techniques in terms of *ex vivo* skin imaging and quantifying are confocal Raman microscopy and MALDI-TOF mass spectrometry imaging (MALDI-TOF MSI). Both techniques were set up, and the semiquantitative skin biodistribution of previously developed dexamethasone (DEX) loaded lipomers was compared using Benzalkonium chloride (BAK) as a tracer of the nanoparticles. In MALDI-TOF MSI, DEX was derivatised with GirT (DEX-GirT) and the semiquantitative biodistribution of both DEX-GirT and BAK was successfully obtained. The amount of DEX measured by confocal Raman microscopy was higher than that measured by MALDI-TOF MSI, but MALDI-TOF MSI proved to be a more suitable technique for tracing BAK. An absorption-promoting tendency of DEX loaded in lipomers versus a free-DEX solution was observed in confocal Raman microscopy. The higher spatial resolution of confocal Raman microscopy (350 nm) with respect to MALDI-TOF MSI (50 μm) allowed to observe specific skin structures like hair follicles. Nevertheless, the faster sampling rate of MALDI-TOF-MSI, permitted the analysis of larger tissue regions. In conclusion, both techniques allowed to simultaneously analyze semiquantitative data together with qualitative images of biodistribution, which is a very helpful tool when designing nanoparticles that accumulate in specific anatomical regions.

1. Introduction

Transdermal drug delivery systems are an interesting alternative for many molecules that are currently administered orally or parenterally (Guy, 2010). Specifically, the vectorization in nanoparticles capable of crossing the stratum corneum and accumulating in skin appendages is a strategy currently used in both the pharmaceutical and cosmetic industries (Raj et al., 2012).

The mechanisms undergone by encapsulated active ingredients and nanoparticles have not yet been fully understood. There are different techniques such as fluorescence confocal microscopy or immunohistofluorescence that allow obtaining qualitative images of the biodistribution of drugs or fluorophores. However, to determine the amount of drug accumulated in the different layers and regions of the skin is still one of the major obstacles that researchers encounter when developing topical drugs.

It is also possible to quantify the non-permeated active ingredient by separation of the skin layers, extraction, and high-performance liquid

* Corresponding authors at: Biomedical Engineering Manager, mesoestetic Pharma Group, s.l. C/ Tecnologia, 25, 08840 Viladecans (Barcelona), Spain (E. Pena-Rodríguez) Universidade de Santiago de Compostela, Pharmacology, Pharmacy and Pharmaceutical Technology department, Praza Seminario de Estudos Galegos, s/n, 15782 Santiago de Compostela, Spain (Francisco J. Otero Espinar).
E-mail addresses: yoleanep@hotmail.com (E. Pena-Rodríguez), francisco.otero@usc.es (F.J. Otero-Espinar).
[1] Present address: Mesoestetic Pharma Group, R&D Department, 08840 Viladecans, Barcelona, Spain.
[2] These authors have contributed equally to this work.
[3] These authors have contributed equally to this work.

https://doi.org/10.1016/j.ijpharm.2023.122808
Received 16 November 2022; Received in revised form 1 March 2023; Accepted 3 March 2023
Available online 6 March 2023

chromatography (HPLC) analysis. Due to the complexity of this technique, only an approximation to the amount of drug penetrated in each layer is achievable, but it is not possible to observe the cutaneous biodistribution of the active ingredient.

Regulatory authorities are becoming increasingly stringent in studying the biodistribution of topical active ingredients, whether for bioequivalence studies, for safety reasons and/or to demonstrate the efficacy of formulations. Thus, advanced analytical techniques that allow selective detection and quantification are needed by the scientific community.

Recently, two reviews have been published on techniques for *ex vivo* imaging and quantification of drug delivery in the skin (Grégoire et al., 2020; Pena et al., 2020). Many of the techniques currently used to analyse the biodistribution of drug treatments require the use of molecular labelling (e.g., fluorescent, or radioactive). Among the label free techniques, confocal Raman microscopy and Matrix Assisted Laser Desorption Ionisation - Time Of Flight Mass Spectrometry Imaging (MALDI-TOF MSI) are two of the techniques with the greatest potential for biomedical analysis of biological tissues(Franzen et al., 2013).

Confocal Raman microscopy is a non-invasive technique with high spatial molecular resolution, up to hundreds of nanometers (Austin et al., 2016; R.J. Silbey, 1995). It is commonly used to study the biodistribution of different compounds within formulations and in different biological tissues. However, the Raman scattering signal is usually weak, requires long acquisition times and can be interfered by tissue autofluorescence. Even so, devices have also been developed to quantify both skin intrinsic molecules and the penetration of different pharmaceutical ingredients in a non-invasive way by *in vivo* confocal Raman (Caspers et al., 2003, 2001).

The first application of MALDI-TOF for skin imaging was performed in 2004 (Bunch et al., 2004). MALDI-TOF MSI allows the analysis of multiple molecules in biological tissues deciphering their spatial biodistribution. Nevertheless, ionically inert or small molecules are difficult to detect by MALDI-TOF. One approach to improve detection sensitivity is to chemically derivatise the molecules of interest and, (Gao et al., 2019; Hong and Wang, 2007; Zhang et al., 2020) in recent years, on-tissue chemical derivatization (OTCD) methods based on the deposition of the derivatization reagents onto the tissue have been developed to improve the MALDI-TOF MSI sensitivity of several molecules like fatty acids, phospholipids, amino acids, steroids etc. (Dueñas et al., 2019; Takeo et al., 2019; Wang et al., 2019; Wu et al., 2016). Although in the past this technique was used to analyse in a qualitative manner (Fitzgerald et al., 1993), the possibility to analyse quantitatively the biodistribution of different molecules has gained interest (Handler et al., 2021). Withal, MSI techniques are generally performed *ex vivo*.

Corticosteroids are one of the most frequently used therapies to treat inflammatory skin diseases. Dexamethasone (DEX) is a corticosteroid commonly used topically to treat diseases such as atopic dermatitis (Yamamoto et al., 2017), ocular inflammation (Saraiya and Goldstein, 2011), and alopecia areata (Leyden and Kligman, 1972). To permeate DEX into skin, different absorption promoters have been used, such as ethanol (at a concentration of 70%) (Yamamoto et al., 2017). Due to the potential adverse effects of ethanol, such as skin irritation or contact dermatitis (Lachenmeier, 2008), structure alteration of the stratum corneum (Kwak et al., 2012) and modification of the skin microbiota (Mcdonnell et al., 1999), it is advisable to minimise its use in topical formulations.

Polymer-lipid hybrid nanoparticles (lipomers) are drug delivery systems with a high loading capacity that could improve the efficacy of DEX in the treatment of diseases occurring in the pilosebaceous unit (i.e., alopecia areata). In previous studies from our group, lipomers were formulated with benzalkonium chloride (BAK) to provide cationic charge and stabilise these nanoparticles against aggregation. Optimised lipomers containing DEX (DEX-lipomers) were physicochemically characterised and their *ex vivo* cutaneous biodistribution in pig skin was qualitatively revealed by confocal fluorescence microscopy and immunohistofluorescence, (Pena-Rodríguez et al., 2021).

The aim of the current research was to go further and studying in a semiquantitative manner the *ex vivo* biodistribution and penetration of topically administered DEX and BAK on human scalp, both in (Pena-Rodríguez et al., 2021) DEX loaded lipomers and as a free-DEX solution. Confocal Raman microscopy and MALDI-TOF MSI application are compared to that purpose.

2. Materials and methods

2.1. Materials

Ethyl cellulose (EC) (Ashland Industries Europe GmbH, Rheinweg, Switzerland), medium-chain triglycerides (MCT) (Oxi-Med Expres S.A., Barcelona, Spain); Tween 80 and Span 60 (Croda Iberica S.A., Barcelona, Spain), and BAK with a relative abundance of the C_{12} and C_{14} homologues of 65.6:35.4 (Sigma Aldrich, St. Louis, MO, USA,) were used to produce the lipomers. DEX (Fagron Ibérica, Barcelona, Spain) was the active pharmaceutical ingredient, and the selected solvents were ethyl acetate (Scharlab S.L., Barcelona, Spain), ethanol absolute (Scharlab), and milli-Q water (In-house). The reagents α-Cyano-4-hydroxycinnamic acid (CHCA), Girards' reagent T (GirT), hematoxylin, eosin, acetic acid, xylene, Canada balsam and phosphate buffer saline (PBS) were purchased from Sigma Aldrich. Trifluoroacetic acid (TFA), acetonitrile and optimal cutting temperature compound (OCT) (Fisher Scientific, Waltham, USA) were used during the sampling and cryo-sections obtention. Methanol (Honeywell Riedel-de Haën, Seelze, Germany) was used during the MALDI-TOF MSI solutions preparation.

2.2. DEX- lipomers manufacturing and physicochemical characterization

The encapsulation of DEX in EC and MCT lipomers was performed by the emulsion solvent evaporation method previously described (Pena-Rodríguez et al., 2021). Briefly, the EC (2.33 % w/w), MCT (0.20 % w/w), DEX (1.00 % w/w), and the surfactant Span 60 (0.16 % w/w) were dissolved in a 15 % w/w organic phase composed of an ethanol: ethyl acetate (1:5) mixture. In parallel, an aqueous phase with Tween 80 (1.50 % w/w), BAK (0.20 % w/w) and milli-Q water (q.s. 100 % w/w) was prepared. Both phases were mixed and emulsified using an UP400st sonicator (Hielscher Ultrasonics, Teltow, Germany) at an amplitude of 40 % for 5 min. Finally, the organic solvent was evaporated under vacuum on a Büchi RII rotary evaporator (BUCHI Ibérica, S.L.U., Barcelona, Spain) at 40 °C for 5 min. Free-DEX solution (1 % w/w) was prepared in a hydroethanolic solution (90:10 w/w, milli Q water: ethanol).

The lipomers obtained were analysed by dynamic light scattering (Zetasizer Nano ZS (Malvern Panalytical, Malvern, UK)). As previously described, DEX-lipomers had a hydrodynamic diameter of 185 ± 5 nm, a polydispersity index of 0.360 ± 0.019, a Z-potential of 39.0 ± 0.1 mV and an encapsulation efficiency of 98.60 ± 0.01 % (Pena-Rodríguez et al., 2021).

2.3. Human scalp in vitro permeation studies

Human scalp was purchased from Biopredic (Saint Grégoire, France), which is authorised for the collection, processing, and sectioning of human biological samples for research purposes. Samples were remnants of surgeries complying with the French law CSP1245-2 with informed consent of the patient, who is anonymised and does not receive financial reward or publicity. The donor was a 58-year-old Caucasian female.

The skin was cleaned with PBS and kept at 4 °C in the same saline solution. Skin pieces were defatted (with a scalpel) and frozen at −20 °C until use. On the day of the experiment, skin pieces were warmed to room temperature and mounted on Franz cells (Vidrafoc, Barcelona, Spain) with an effective diffusion area of 0.196 cm^2 and around 12 mL of

receptor volume capacity (PBS at 32 °C and stirred at 500 rpm). An amount of 76 mg of DEX-lipomers or free-DEX formulations were applied in infinite doses and non-occluded conditions (Lau and Ng, 2017). Untreated skin was also included to study possible interferences and to deposit the standards on tissue. After 18 h of permeation, the diffusion surface was washed with PBS, the edges of the skin pieces were cut with a scalpel and discarded, and the area in contact with the formulation was frozen in dry ice immediately before use.

2.4. Tissue cryosectioning and histology

Carefully using a small drop of OCT to avoid any contamination, the skin pieces were attached to the cryostat holder (Leica CM 3050 S (Leica Biosystems, Barcelona, Spain)). Working at a temperature of −27 °C, skin cross-sections with a 12 μm thickness were collected in different types of slides. On the same slide, sections of different tissues were included: non-permeated, permeated with DEX-lipomers and permeated with free-DEX. Calcium fluoride (CaF_2) slides (Crystan Ltd, Poole, UK) were used for confocal Raman microscopy, and indium tin oxide (ITO)-coated slides (Bruker Daltonics, Germany) for MALDI-TOF MSI. Skin cryosections were then dried overnight under vacuum and kept at −80 °C.

Additionally, consecutive tissue sections to those cut for MALDI-TOF MSI were also collected on Superfrost™ poly-lysine-coated slides (Fisher Scientific) with histological purposes. Hematoxylin & eosin staining was performed following the standard procedure. Briefly, slides were immersed for 2 min in 100 %, 90 %, 80 % and 70 % ethanol, consecutively. Then, the samples were washed in milli-Q water for 5 min. Afterwards, slides were immersed in hematoxylin for 8 min and washed again with milli-Q water. The next step was to dehydrate the samples for 3 min in 70 %, 80 % and 90 % increasing ethanol solutions before being submerged for 2 min in an eosin solution and washed for 3 min with 90 % ethanol. Finally, the slides were immersed in xylene (5 min, twice) and mounted with Canada balsam. Optical images were obtained in a Leica Z16 APO vertical fluorescence stereomicroscope with a 1x magnification (Leica Microsystems, Wetzlar, Germany).

2.5. Semiquantification curves preparation

Mixtures of DEX and BAK were prepared in 80 % w/w methanol and 0.2 % w/w TFA at four different concentrations (Table 1). Drops (0.5 μl) of these mixtures were placed on untreated skin cryosections and were left to dry for 20 min in the flow hood, before conducting imaging analyses.

The signal intensities contained in the regions of interest (ROIs) where the droplets had previously been deposited were obtained with WItec Suite Five + version 5.3 (WITec, Ulf, Germany) and FlexImaging 3.0 (Bruker Daltonics, Bremen, Germany) softwares for confocal Raman microscopy and MALDI-TOF MSI respectively. These data were employed to obtain regression curves (Figures S1-S4 in supplementary data), corrected by the area of each ROI measured with ImageJ software.

Linear regressions were performed using Microsoft Excel™ software (Microsoft Corporation, Washington, USA).

Table 1
DEX and BAK concentrations and corresponding amounts in a 0.5 μl drop for each of the standards.

DEX (ng/μl)	BAK (% w/w)	DEX (ng)	BAK (ng)
2000	2E-3	1000	10
200	2E-4	100	1
20	2E-5	10	1E-1
2	2E-6	1	1E-2

2.6. Confocal Raman microscopy analysis

Tissue cross-sections were analysed with an Alpha 300R confocal Raman microscope (WITec), configurated with a 20x Zeiss EC Epiplan-Neofluar objective, a 633 nm laser and a 600 lines/mm grating. Results were treated with Project Five Plus 5.3 software (WITec).

Optical images of the tissues were obtained, then, the ROIs to be scanned were defined and Raman spectra were obtained. Scanned areas were composed of 100 lines per area, and 1000 points per line with a laser power of 10 mW. The live auto focus tool was selected to follow the sample topography in real time.

Once the data were obtained, cosmic ray removal was carried out for each analysis with a filter size of 3 and a dynamic factor of 8. A background subtraction was performed with a polynomial of degree 6 making sure that no band was detrened. After the correction of the spectrum, WItec true component analysis tool was performed to calculate the principal components of the spectra. All these data processing steps were performed using WItec Suite Five Plus 5.3 (WITec). This method considers the full Raman spectra rather than single bands. This tool is based on an algorithm that describes each measured spectrum of a hyperspectral dataset by a linear combination of reference spectra (Benito-González et al., 2020). Then, the biodistribution map of the DEX was superimposed on the optical image of the tissue using the software's "overlay" tool.

The formula to convert from skin volume to skin mass is shown in equation (1), where $M_{scanned}$ is the mass of the scanned region (μg), T is the thickness of the skin sample (cm), and ρ is the skin density (1 g/cm^3).

$$M_{scanned}(\mu g) = A \times T \times \rho \times 10^{-6} \quad (1)$$

The semiquantitative analysis was performed using the regressions lines obtained with the standards.

2.7. MALDI-TOF MSI set-up

To optimise the experimental conditions for DEX detection by MALDI-TOF MS as a preliminary step to MSI experiments, different ionization tests were performed. These tests consisted of studying the feasibility to analyze DEX, BAK, checking the effect of derivatization with GirT, and making sure that no interferences between the different compounds were generated. Underivatised samples of 2 μg/μl DEX, 100 pg/μl GirT reagent, 0.2% w/w BAK and 1:1 mixture of GirT (100 pg/μL): BAK (2 μg/μl) were analyzed.

DEX was derivatised in solution as a strategy to increase sensitivity. Two stock solutions consisting of 4 μg/μl DEX in acetic acid: methanol (10:90), and 2 μg/μl GirT in milli-Q water were prepared. Then, 200 μl of the DEX stock and 10 μl of the GirT stock were mixed and incubated at 37 °C for 5 min.

Once individual spectra were obtained, a 1:1 mixture of GirT (50 pg) with BAK 0.2 % w/w and a 2-μg sample of GirT-DEX conjugate were analysed to study the selectivity.

2.8. MALDI-TOF MSI analysis

On-tissue chemical derivatization (OTCD) was required for DEX detection. For this purpose, ITO slides containing skin cryosections, were sprayed with a 5 mg/mL solution of GirT in 80 % methanol, 20 % milli-Q water and 0.2 % TFA using the ImagePrep™ device (Bruker). The optimised set-up for OTCD was 40 cycles, at 40 % power, with 2.2 s spray pulse, 30 s incubation and 60 s of drying per cycle. The amount of the derivatizing agent was calculated by weight difference before and after spraying (average deposited GirT: 1.78 μg/mm^2). The slides were then placed in a glass Petri dish with moistened paper and incubated at 40 °C for 1 h (Guo et al., 2020). Afterwards, the slides were dried under vacuum for 30 min.

Then, samples were sprayed with CHCA (10 mg/ml in 80 %

acetonitrile, 20 % milli-Q water and 0.2 % TFA) as MALDI matrix using ImagePrep™. A thickness parameter of 2/3 and tune of 0% were selected in the CHCA standard method (average deposited CHCA: 1.40 μg/mm^2). High resolution (6400 dpi) optical images of the ITO slides were obtained with an Epson Perfection V600 scanner (Epson Ibérica, Barcelona, Spain). Slides were kept in dark until MSI analysis.

Tissue slides were finally mounted into the MTP slide adapter (Bruker) and placed into the MALDI-TOF mass spectrometer (UltrafleXtreme, Bruker). Internal calibration was performed with a 1:1:1 mixture of in-solution GirT-derivatised DEX (2000 ng/μl), BAK (20 ng/μl), and CHCA (10 μg/μl) deposited on the ITO slide after spraying the matrix.

Using FlexImaging™ 3.0 and FlexControl™ 3.4 softwares (Bruker), MSI data from permeated skin cross sections were obtained in reflector positive ion mode at a mass range of 240–800 *m/z*. The laser intensity was set to 85 % and its diameter to the medium size, which corresponds with a spatial resolution of 50 μm. Ion extraction time was set at 100 ns. The spectra were averaged from 500 laser shots per spot, in random spots mode. The mass error was < 50 ppm. When DEX and BAK standards were analysed for quantitation purposes, the laser was used at 60 % power, large diameter, and fast mode, to avoid signal saturation. A total ion count (TIC) normalization was automatically performed by dividing the intensities of each *m/z* by the mean of intensities of the mean spectrum. In this way, the ion density maps to visualise the spatial distribution of each targeted *m/z* (506.3, 304.3 and 332.3 for DEX, BAK C_{12} and BAK C_{14} respectively) in each sample was obtained in FlexImaging™.

Analogous to the confocal Raman studies, semiquantitative analysis was also performed using the regression lines obtained with the MALDI-TOF MSI standards.

3. Results and discussion

The steps necessary to study the cutaneous biodistribution of DEX and BAK by confocal Raman microscopy and MALDI-TOF MSI are summarised in Fig. 1. The first step was to permeate the experimental formulations with free-DEX or DEX-lipomers in human scalp explants using Franz cells. Once permeated, skin cryosections were obtained for histology, confocal Raman microscopy and MALDI-TOF MSI. Known amounts of DEX and BAK were deposited on-tissue to perform the semiquantitative analysis by Confocal Raman and MALDI-TOF MSI. In the case of MSI analysis, DEX was derivatised on tissue to increase its sensitivity (Zhang et al., 2020). Finally, the results were interpolated to obtain semiquantitative biodistribution maps.

3.1. Semiquantification of DEX penetrating human skin by confocal Raman microscopy

First, the individual spectra of untreated human scalp, BAK, DEX, DEX-lipomers and a mixture of DEX and BAK (1:1) deposited on untreated human scalp, were obtained by means of Confocal Raman (Fig. 2A). The objective of this first step was to test the feasibility to trace DEX and BAK in the different matrices. Possible band overlaps with both human scalp and lipomer excipients were checked. The spectra of free-DEX and BAK are characterised by intense peaks at 1656 cm^{-1} ("John Wiley & Sons, Inc. SpectraBase; https://spectrabase.com/spectrum/GhWXEmhuBn8 (accessed 19/1/2023).," n.d.), and at 1007 cm^{-1} ("John Wiley & Sons, Inc. SpectraBase; https://spectrabase.com/ad?a = SPECTRUM_1sk1IH8Yu2l&r = https://spectrabase.com/spectrum/1sk1IH8Yu2l (accessed 19/1/2023).," n.d.), respectively (Fig. 2A),. By comparing the spectra of untreated human scalp and human scalp with the mixture of DEX and BAK, the possibility of tracing the DEX peak in the skin but not BAK was proven. Due to the overlap with the phenylalanine peak (symmetric ring breathing at approximately 1004 cm^{-1}) present in the skin (Hernández et al., 2013), the low signal of the peak, and the low concentration of BAK relative to DEX in the nanoparticles (10 times less), it was not possible to detect it by confocal Raman.

A filter was created at 1656 cm^{-1} with a peak width of 50 cm^{-1} and 4

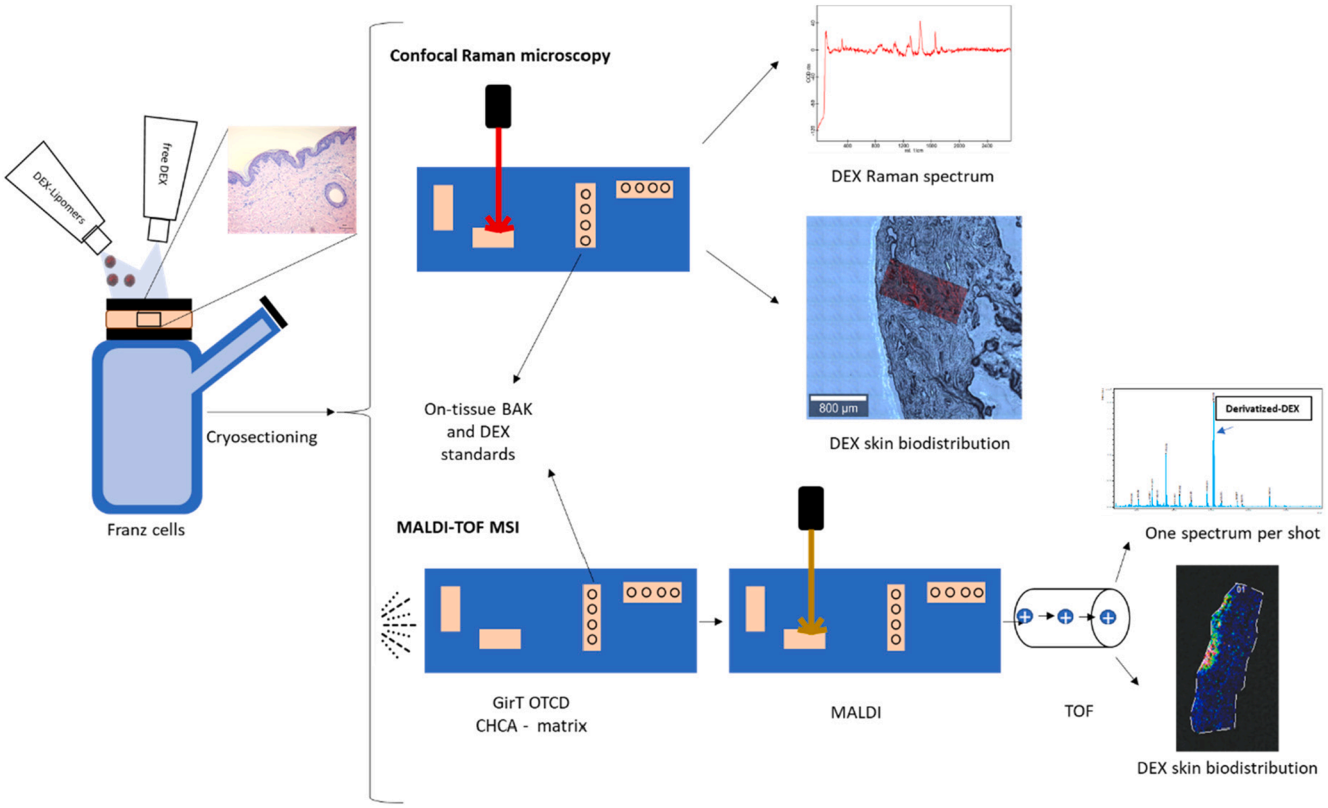

Fig. 1. Steps on the study of the cutaneous biodistribution of DEX and BAK by confocal Raman spectroscopy and MALDI-TOF MSI.

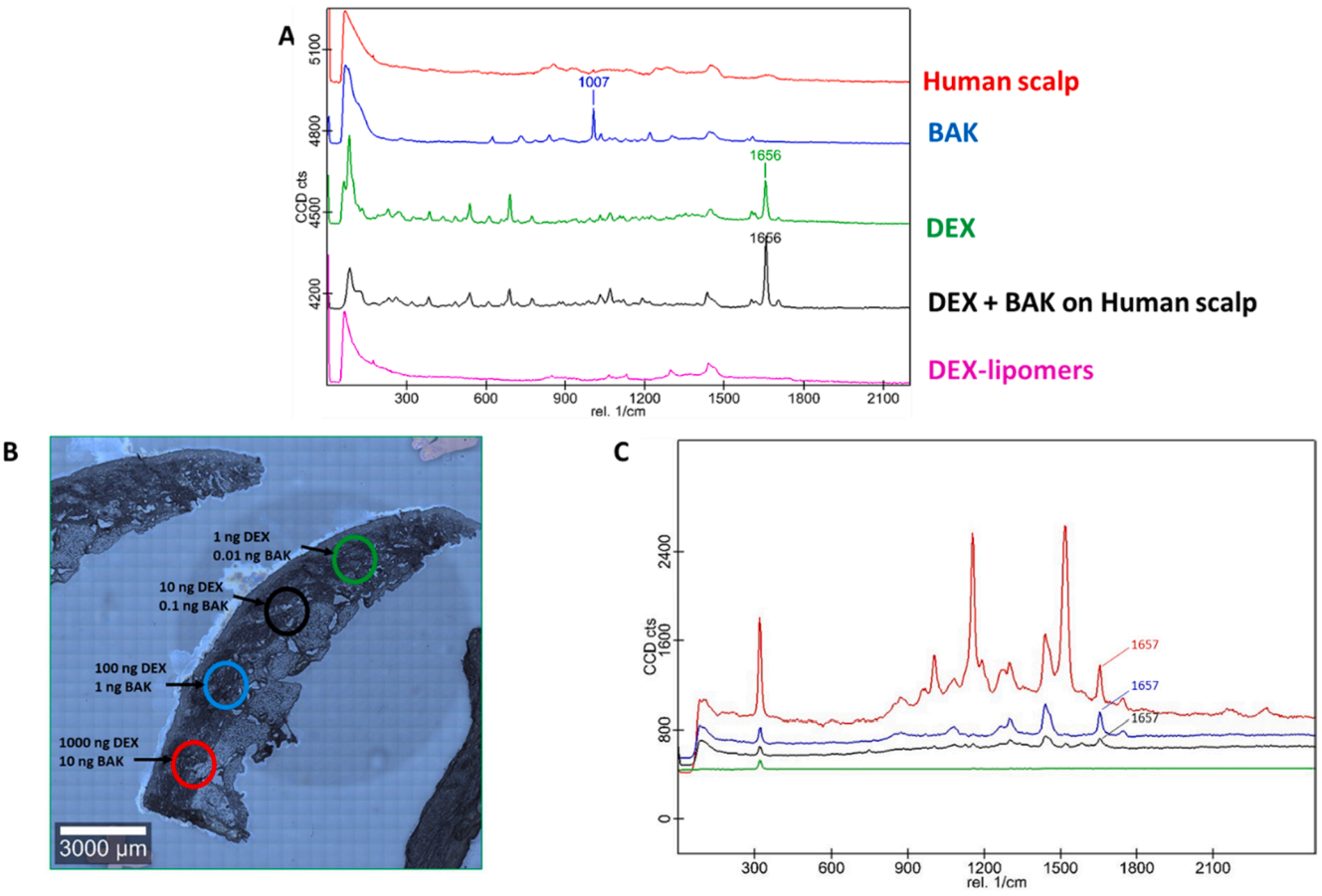

Fig. 2. (A) Individual Raman spectra of human scalp (red), BAK (blue), DEX (green), and a mixture of DEX and BAK (1:1) deposited on human scalp (black), and DEX-lipomers (pink). (B) Untreated human scalp cryosection showing the different droplets for the quantification curve: 1000 ng DEX and 10 ng BAK (red), 100 ng DEX and 1 ng BAK (blue), 10 ng DEX and 0.1 ng BAK (black), 1 ng DEX 0.01 ng and BAK (green). (C) Raman spectra of the ROIs scanned for each standard (same colours as before) showing the 1656 cm^{-1} DEX characteristic Raman peak. (For interpretation of the references to colour in this figure legend, the reader is referred to the web version of this article.)

points were taken on each side to obtain the average intensity sum of each standard. The standard curve of DEX and the corresponding equation are shown in supplementary data Figure S1.

When permeated human scalp was analysed (Fig. 3), it was possible to detect lipomer-delivered DEX at > 1000 µm depths (Fig. 3A). By observing the hair follicles, DEX accumulation can be seen in the outer root sheath of the follicle. In previous studies (Pena-Rodríguez et al., 2021) the accumulation of DEX in hair follicles and sebaceous glands was also observed by immunohistofluorescence techniques when it was loaded in lipomers.

In addition to qualitative biodistribution, a semiquantitative estimate of the amount of DEX present in the scanned skin regions was obtained. After interpolation with the standard curves a DEX amount of 36.25 ± 11.79 ng/µg skin was detected in tissues permeated with free-DEX, whereas 51.32 ± 22.06 ng/µg skin were quantified in skin treated with DEX lipomers. Although there was a substantial increase in DEX penetrance when using lipomers, when DEX amount was corrected with equation (1) no significant differences were found (p-value = 0.22, Fig. 3C).

When qualitatively comparing the amounts of DEX in different scanned regions of the skin, it was found that in the free-DEX solution, the active ingredient mainly accumulates in superficial layers (epidermis and stratum corneum) (Fig. 3B), while when encapsulated in lipomers, accumulation was observed around follicles and in the dermis at a depth of up to approximately 1000 µm (Fig. 3A).

3.2. MALDI-TOF MSI set-up

The spectrum of DEX (supplementary data Figure S5A) showed very low intensity peaks at m/z = 393.2 Da corresponding to the mass of protonated DEX ($M + H^+$). Low intensity peaks of DEX + Na^+ and DEX + K^+ are also shown. This indicated the need to derivatise DEX to increase the signal intensity. As for BAK, being a quaternary ammonium salt, the signal obtained was much more intense and suitable for tracing lipomers by MALDI-TOF MSI. The peaks corresponding to the BAK C_{12} (m/z = 304.3 Da) and BAK C_{14} analogs (m/z = 332.3 Da) can be observed (supplementary data Figure S5B). The spectrum of supplementary data Figure S5C shows the GirT peak at m/z = 132.1 Da.

The reaction scheme between aldehydes/ketones with GirT reagent is shown in supplementary data Figure S6A. Although attack on either group 3 and 20 ketone of DEX would be possible, it was assumed that the 20 ketone was more prone to nucleophilic attack by the hydrazide than the ketone in the 1,4-diene-20-one system of the pregnane structure (Figure S6B). The GirT added 114 Da to the DEX molecule, and consequently the derivatised DEX peak was observed at 506.3 Da.

As can be seen in supplementary data Figure S7 A, there were no changes in the spectrum when mixing GirT and BAK, so no reaction seems to be possible between these two molecules. The method is considered selective, as no interferences between reagents or different compounds were observed.

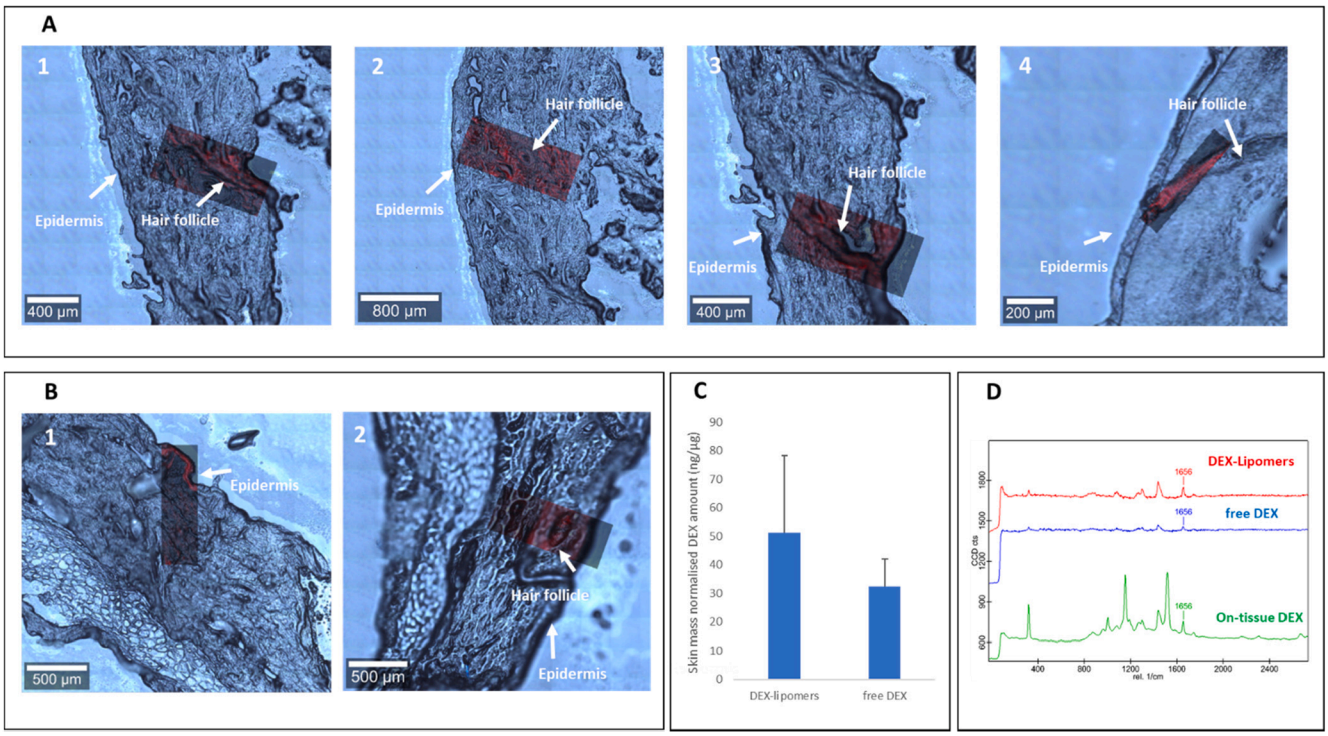

Fig. 3. DEX-lipomers and free-DEX permeated human scalp cryosections analysis by confocal Raman microscopy. (A) DEX-lipomers permeated cryosections, showing the overlay of the DEX distribution map on the scanned regions number A.1, A.2, A.3, and A.4. (B) Free-DEX permeated cryosections, showing the overlay of the DEX distribution map on the scanned regions B.1 and B.2. White arrows indicate the localization of epidermis and hair follicles in the cryosections (C) DEX-lipomers (n = 4) and free-DEX (n = 2) skin mass normalised DEX amount (ng/µg) bar diagram. (D) DEX Raman spectra of on-tissue DEX standard (green), DEX lipomers (red), and free-DEX (blue). (For interpretation of the references to colour in this figure legend, the reader is referred to the web version of this article.)

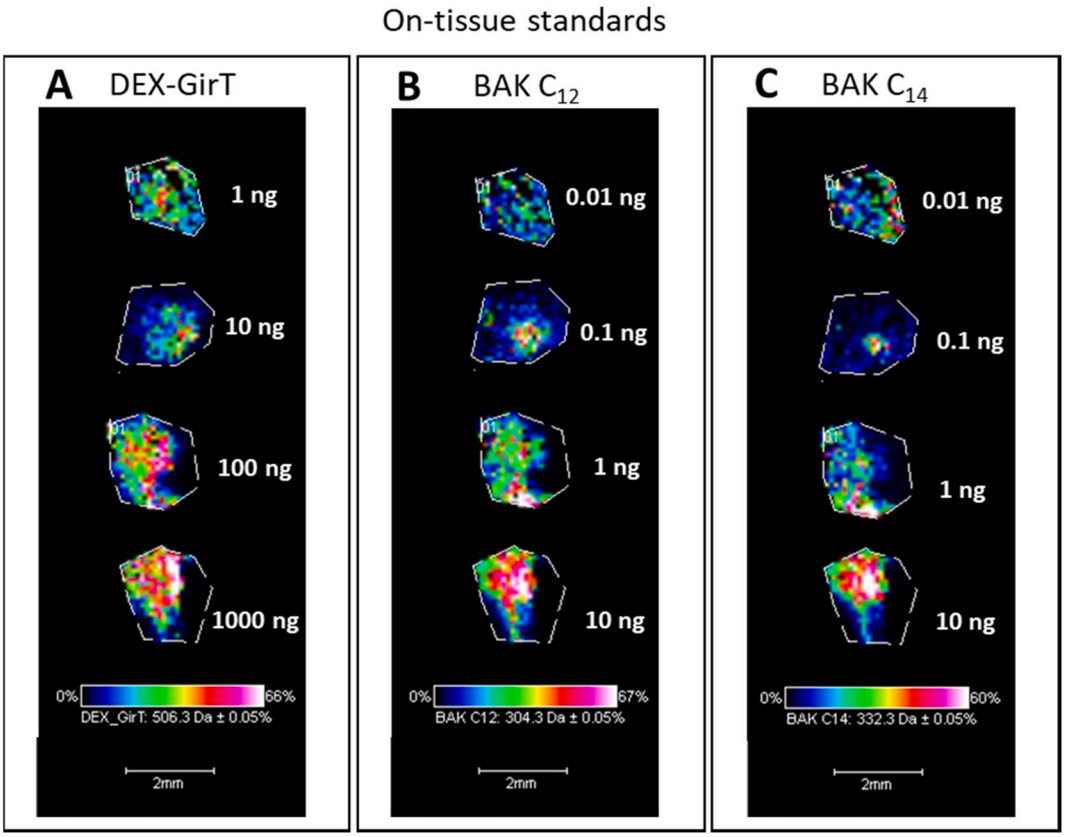

Fig. 4. On-tissue m/z = 506.3 Da DEX-GirT (A), m/z = 304.3 Da BAK C_{12} (B) and m/z = 332.3 BAK C_{14} (C) standards intensity maps after MALDI-TOF MSI analysis. Scale bars (2 mm) and intensity colour scale bars are shown, white text indicates the corresponding amount of each standard.

3.3. Semiquantification of DEX and BAK penetrated into human skin by MALDI-TOF MSI

A known drawback for MALDI-TOF MSI is the analyte ion suppression phenomena produced by the tissue matrix and other interferences (Rzagalinski and Volmer, 2017; Signor et al., 2007). To counter this problem, standards can be deposited on blank tissue and signals obtained used to correct the matrix effect in the samples (Goodwin et al., 2011).

Quantitative, reproducible derivatization of the tissue permeated material can be affected by the tissue characteristics, incubation conditions, and reagent and matrix concentration and spraying conditions (Barré et al., 2016). On the basis of previous studies (Guo et al., 2020; Zhang et al., 2020) we tuned these parameters for the better response in our hands. OTCD with GirT was performed (Fig. 4). Standard curves were obtained for the three analytes, representing the logarithm of the intensity of the corresponding peak as a function of the logarithm of the amount of standard deposited on tissue. (Figures S2 - S4 in supplementary data).

MALDI-TOF MSI images of the DEX-lipomers and free-DEX permeated human scalp tissues showed the distribution of derivatised DEX in the skin cryosections. In addition, BAK biodistribution allowed to trace the lipomers (Fig. 5). The derivatised-DEX signal at *m/z* 506.3 Da confirmed adequate derivatization of DEX. As can be seen, there is an accumulation of DEX in the more superficial layers (epidermis) and the amount of DEX in the dermis and deeper layers is lower. Fig. 5 B correspond to free-DEX permeated tissues, with a similar biodistribution as the lipomers.

In previous immunohistofluorescence studies (Pena-Rodríguez et al., 2021), when DEX was loaded in lipomers instead of in a free control

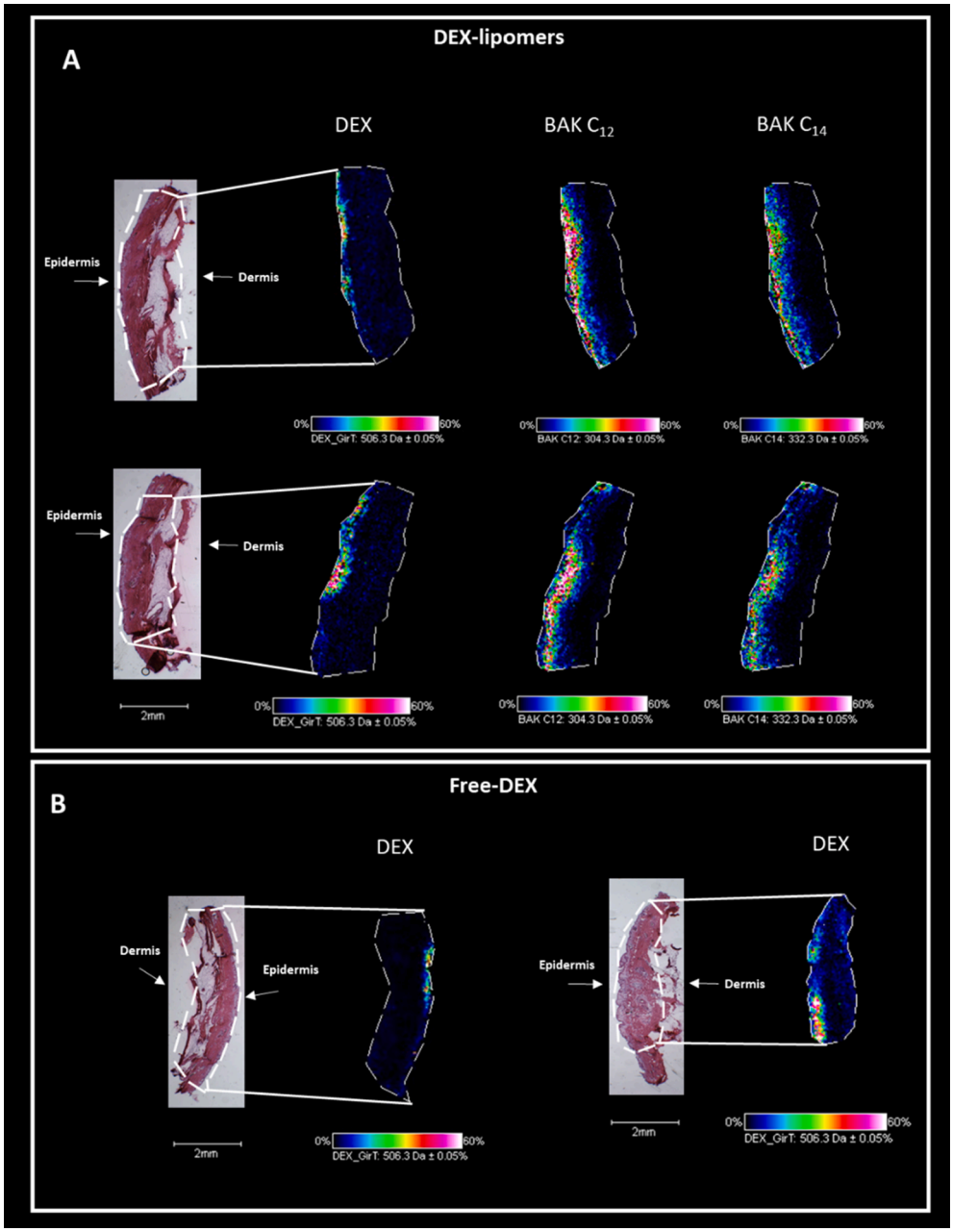

Fig. 5. MALDI-TOF MSI biodistribution maps and histological cryosections of: (A) DEX, BAK C_{12}, and BAK C_{14} after DEX-lipomers permeation on human scalp. (B) DEX after free-DEX permeation on human scalp. White arrows indicate the epidermis and dermis orientation on the slices. Scale and intensity bars are shown in each panel. Overlaying of the ROIs in the corresponding histological cryosections is also shown in each histological image.

solution, its skin penetration capacity was higher. MALDI-TOF MSI results have not shown these differences, probably, due to the lower spatial resolution of MALDI-TOF MSI set-up (50 μm), where it was not possible to differentiate biodistribution in hair follicles.

Simultaneously, the biodistribution of BAK C_{12} and BAK C_{14} in skin tissues permeated with DEX-lipomers was also analysed. The biodistribution results seem to indicate that the lipomers were able to permeate beyond the epidermis (up to about 800 μm depth) (Fig. 5A). This would agree with the results obtained in previous studies (Pena-Rodríguez et al., 2021). In those studies, it was observed that by encapsulating a hydrophobic fluorophore (Coumarin 6) and labelling the lipomers with Lissamine™ Rhodamine B, the lipomers were shown to penetrate deep layers, releasing the encapsulated active ingredient in epidermis and hair follicles.

The results were also normalised by the amount of skin analysed (in μg) to compare them with the results obtained by confocal Raman. The total amount of DEX-GirT extracted from the skin tissues was similar in the case of DEX-lipomers (0.155 ± 0.064 ng/μg skin) and free-DEX (0.163 ± 0.069 ng/μg skin). It was observed that the DEX biodistribution was similar with both formulations, and it was accumulated in the most superficial layers of the skin. It would appear that BAK C_{12} penetrated in greater quantities than BAK C_{14} (0.017 ± 0.000 versus 0.005 ± 0.001 ng/μg skin respectively). However, the relative abundance of the BAK C_{12} homologue in bulk BAK was higher than that of BAK C_{14} (Kampf, 2018), which seems to explain the differences found.

Several authors studied the accumulation of DEX loaded into 100–200 nm positively charged EC nanoparticles by skin layer separation and quantification. These investigators performed permeations at a lower DEX dose (0.05%) and at shorter times (6–8 h permeation) (Balzus et al., 2017; Beber et al., 2016; Döge et al., 2016). For this reason, at a quantitative level, it is difficult to make an adequate comparison with our results. Nevertheless, the studies in the literature showed accumulation in epidermis when DEX was loaded in EC polymeric nanoparticles, which agrees with the results observed in Fig. 5A.

3.4. Confocal Raman and MALDI-TOF MSI comparison

A summary table (Table 2) of the two techniques applied to the semiquantitative biodistribution of DEX and BAK after permeation in the human scalp is shown below.

Confocal Raman has proven to be a very useful technique to study and compare the cutaneous biodistribution of DEX in a semiquantitative manner. When analyzing the results obtained through both techniques, the amounts of DEX detected in MALDI-TOF MSI were lower (0.155 ± 0.064 in MALDI-TOF MSI versus 51.32 ± 22.06 ng/μg in confocal Raman for DEX-lipomers). A possible explanation is the fact that quantification in this case is performed indirectly, through on-tissue derivatization with GirT. Since these are permeated samples, it is possible that the derivatization yield is lower than in the case of calibrators, where DEX is more accessible when deposited onto the cross section. In addition, another issue for quantification with mass spectrometry is the matrix effect. A competition between the analyte and other ionised molecules from the matrix could take place (Grégoire et al., 2020). The matrix effect present in MALDI-TOF MSI, and the ionization efficiency of DEX-GirT may also be a cause of the lower amount of DEX detected with respect to confocal Raman.

Table 2
MALDI-TOF MSI versus Confocal Raman comparison for skin imaging analysis.

	MALDI-TOF MSI	Confocal Raman
Spatial resolution	30–50 μm (equipment used in this research)	350 nm
Sampling time	1–2 h	10–15 h
Setting-up complexity	Harder	Easier
Analysis type	Destructive	Non-destructive
Interferences	Matrix effect (ion suppression during matrix desorption)	Skin autofluorescence
DEX sensitivity	Lower	Higher
BAK sensitivity	Higher	Lower

One of the major differences between the characteristics of the two techniques with the set-up used in these experiments was the spatial resolution. With the equipment used in this work, a spatial resolution of 350 nm by Confocal Raman and 50 μm by MALDI-TOF MSI was achieved. This higher resolution makes it possible to observe hair follicles, which was not possible with 50 μm resolutions. It was possible to reduce the diameter of the MALDI-TOF MSI laser to 30 μm but the intensities obtained at this resolution were too low. However, nowadays there are new generation MALDI-TOF MSI equipment that allow to achieve better spatial resolutions (of up to 300 nm) (Meng et al., 2020).

Due to low scattering efficiency, Raman microscopy is a time-consuming technique with a rather slow sampling rate (Ryabchykov et al., 2018). For this reason, the ROIs analysed in this work using MALDI-TOF MSI covered practically 100% of the tissue to be analysed (Fig. 5), while the regions analysed using confocal Raman were considerably smaller (Fig. 3). The set-up of MALDI-TOF MSI is more complex than for confocal Raman. Although the sampling time once the technique is optimised is shorter in MALDI-TOF MSI, the time and complexity required to prepare the samples is greater due to the need to establish the different steps described in section 3.2 MALDI-TOF MSI set-up.

Another difference is the type of signal interferences encountered in each technique. Skin autofluorescence is the main interference in confocal Raman microscopy, while in MALDI-TOF MSI, the sensitivity, ionization, and the ability to derivatise biomolecules can be different depending on the different MALDI matrices used (Perry et al., 2020). Unlike MALDI-TOF MSI, confocal Raman microscopy is a non-destructive technique, which has allowed the development of devices for *in vivo* skin permeation analysis (Caspers et al., 1998). However, both techniques are complementary when analysing biological tissues. In terms of sensitivity for each analysed compound, while for DEX the sensitivity was higher in confocal Raman microscopy, BAK was only detected by MALDI-TOF MSI. The higher sensitivity for BAK in MALDI-TOF MSI is given by the cationic character of the quaternary ammonium group in the compound.

4. Conclusion

MALDI-TOF MSI and confocal Raman microscopy techniques were set up and compared to obtain semiquantitative data on the cutaneous biodistribution of DEX and BAK after permeation of DEX-lipomers versus a free-DEX control solution. The DEX biodistribution obtained with confocal Raman agree with previous studies performed also on DEX-lipomers by qualitative immunohistofluorescence techniques where a penetration-promoting tendency was observed when loaded in the nanoparticles (Pena-Rodríguez et al., 2021). A detailed comparison of both techniques leads to the conclusion that they are complementary techniques. MALDI-TOF MSI is very useful when analysing larger tissue regions, while confocal Raman microsocpy allows to obtain higher spatial resolutions comparing to MALDI-TOF MSI conventional equipments. New equipment based on MSI with higher spatial resolutions are appearing, so the prospects for this technology are very promising. The possibility of obtaining qualitative maps of the biodistribution of compounds and combining it with quantitative data is a very helpful tool for developing drug delivery systems that accumulate in specific anatomical regions. Further work needs to be done on the validation of the quantification method, increasing the number of replicates and standard curve points for both techniques to obtain robust quantiative data with different molecules.

CRediT authorship contribution statement

Eloy Pena-Rodríguez: Investigation, Methodology, Formal analysis, Data curation, Writing – original draft, Visualization. **Teresa García-Berrocoso:** Investigation, Validation, Writing – original draft, Visualization. **Ezequiel Vázquez Fernández:** Investigation, Validation, Methodology. **Francisco J. Otero-Espinar:** Resources, Formal analysis, Writing – review & editing, Visualization, Supervision. **Joaquin Abian:** Conceptualization, Resources, Writing – review & editing, Supervision, Project administration, Funding acquisition. **Francisco Fernández-Campos:** Conceptualization, Resources, Writing – review & editing, Supervision, Project administration, Funding acquisition.

Declaration of Competing Interest

The authors declare the following financial interests/personal relationships which may be considered as potential competing interests: [Pena E. reports financial support was provided by Government of Catalonia. Garcia T. reports equipment, drugs, or supplies was provided by Spain Ministry of Science and Innovation.].

Data availability

Data will be made available on request.

Acknowledgements

This research received funding from the Generalitat de Catalunya Industrial Doctorate program of Eloy Pena Rodríguez, expedient number 2019 DI 1989691. Teresa García-Berrocoso holds a grant PTA2018-016332-I funded by MCIN/AEI /10.13039/501100011033. Assistance provided by Elena Bailo from WITec GmbH was greatly appreciated.

Appendix A. Supplementary material

Supplementary data to this article can be found online at https://doi.org/10.1016/j.ijpharm.2023.122808.

References

Austin, L.A., Osseiran, S., Evans, C.L., 2016. Raman technologies in cancer diagnostics. Analyst. https://doi.org/10.1039/c5an01786f.

Balzus, B., Sahle, F.F., Hönzke, S., Gerecke, C., Schumacher, F., Hedtrich, S., Kleuser, B., Bodmeier, R., 2017. Formulation and ex vivo evaluation of polymeric nanoparticles for controlled delivery of corticosteroids to the skin and the corneal epithelium. Eur. J. Pharm. Biopharm. 115, 122–130. https://doi.org/10.1016/j.ejpb.2017.02.001.

Barré, F.P.Y., Flinders, B., Garcia, J.P., Jansen, I., Huizing, L.R.S., Porta, T., Creemers, L. B., Heeren, R.M.A., Cillero-Pastor, B., 2016. Derivatization strategies for the detection of triamcinolone acetonide in cartilage by using matrix-assisted laser desorption/ionization mass spectrometry imaging. Anal Chem 88, 12051–12059. https://doi.org/10.1021/acs.analchem.6b02491.

Beber, T.C., de Andrade, D.F., dos Santos Chaves, P., Pohlmann, A.R., Guterres, S.S., Ruver Beck, R.C., 2016. Cationic polymeric nanocapsules as a strategy to target dexamethasone to viable epidermis: Skin penetration and permeation studies. J. Nanosci. Nanotechnol. 16, 1331–1338. https://doi.org/10.1166/jnn.2016.11670.

Benito-González, I., Martínez-Sanz, M., López-Rubio, A., Gómez-Mascaraque, L.G., 2020. Confocal Raman imaging as a useful tool to understand the internal microstructure of multicomponent aerogels. J. Raman Spectrosc. 51, 2022–2035. https://doi.org/10.1002/jrs.5936.

Bunch, J., Clench, M.R., Richards, D.S., 2004. Determination of pharmaceutical compounds in skin by imaging matrix-assisted laser desorption/ionisation mass spectrometry. Rapid Commun. Mass Spectrom. 18, 3051–3060. https://doi.org/10.1002/rcm.1725.

Caspers, P.J., Lucassen, G.W., Wolthuis, R., Bruining, H.A., Puppels, G.J., 1998. In Vitro and In Vivo Raman Spectroscopy of Human Skin. Biospectroscopy 4, 31–39.

Caspers, P.J., Lucassen, G.W., Carter, E.A., Bruining, H.A., Puppels, G.J., 2001. In Vivo Confocal Raman Microspectroscopy of the Skin: Noninvasive Determination of Molecular Concentration Pro®les. J Invest Dermatol 116, 434–442.

Caspers, P.J., Lucassen, G.W., Puppels, G.J., 2003. Combined in vivo confocal Raman spectroscopy and confocal microscopy of human skin. Biophys J 85, 572–580. https://doi.org/10.1016/S0006-3495(03)74501-9.

Döge, N., Hönzke, S., Schumacher, F., Balzus, B., Colombo, M., Hadam, S., Rancan, F., Blume-Peytavi, U., Schäfer-Korting, M., Schindler, A., Rühl, E., Skov, P.S., Church, M.K., Hedtrich, S., Kleuser, B., Bodmeier, R., Vogt, A., 2016. Ethyl cellulose nanocarriers and nanocrystals differentially deliver dexamethasone into intact, tape-stripped or sodium lauryl sulfate-exposed ex vivo human skin - assessment by intradermal microdialysis and extraction from the different skin layers. J. Control. Release 242, 25–34. https://doi.org/10.1016/j.jconrel.2016.07.009.

Dueñas, M.E., Larson, E.A., Lee, Y.J., 2019. Corrigendum: Toward Mass Spectrometry Imaging in the Metabolomics Scale: Increasing Metabolic Coverage Through Multiple On-Tissue Chemical Modifications (Frontiers in Plant Science, (2019), 10, 10.3389/fpls.2019.00860). Front Plant Sci. 10.3389/fpls.2019.01079.

Fitzgerald, M.C., Parr, G.R., Smith', L.M., 1993. Basic Matrices for the Matrix-Assisted Laser Desorption/ Ionization Mass Spectrometry of Proteins and Oligonucleotides, Anal. Chem.

Franzen, L., Selzer, D., Fluhr, J.W., Schaefer, U.F., Windbergs, M., 2013. Towards drug quantification in human skin with confocal Raman microscopy. Eur. J. Pharm. Biopharm. 84, 437–444. https://doi.org/10.1016/j.ejpb.2012.11.017.

Gao, X., Lu, Y., Wei, M., Yang, M., Zheng, C., Wang, C., Zhang, Y., Huang, L., Wang, Z., 2019. Matrix-Assisted Laser Desorption/Ionization Time-of-Flight Mass Spectrometry Analysis of Human Milk Neutral and Sialylated Free Oligosaccharides Using Girard's Reagent P On-Target Derivatization. J. Agric. Food Chem. 67, 8958–8966. https://doi.org/10.1021/acs.jafc.9b02635.

Goodwin, R.J.A., MacKay, C.L., Nilsson, A., Harrison, D.J., Farde, L., Andren, P.E., Iverson, S.L., 2011. Qualitative and quantitative MALDI imaging of the positron emission tomography ligands raclopride (a D2 dopamine antagonist) and SCH 23390 (a D1 dopamine antagonist) in rat brain tissue sections using a solvent-free dry matrix application method. Anal. Chem. 83, 9694–9701. https://doi.org/10.1021/ac202630t.

Grégoire, S., Luengo, G.S., Hallegot, P., Pena, A.M., Chen, X., Bornschlögl, T., Chan, K.F., Pence, I., Obeidy, P., Feizpour, A., Jeong, S., Evans, C.L., 2020. Imaging and quantifying drug delivery in skin – Part 1: Autoradiography and mass spectrometry imaging. Adv. Drug Deliv. Rev. https://doi.org/10.1016/j.addr.2019.11.004.

Guo, S., Tang, W., Hu, Y., Chen, Y., Gordon, A., Li, B., Li, P., 2020. Enhancement of On-tissue Chemical Derivatization by Laser-Assisted Tissue Transfer for MALDI MS Imaging. Anal. Chem. 92, 1431–1438. https://doi.org/10.1021/acs.analchem.9b04618.

Guy, R.H., 2010. Transdermal drug delivery. Handb Exp. Pharmacol. https://doi.org/10.1007/978-3-642-00477-3_13.

Handler, A.M., Pommergaard Pedersen, G., Troensegaard Nielsen, K., Janfelt, C., Just Pedersen, A., Clench, M.R., 2021. Quantitative MALDI mass spectrometry imaging for exploring cutaneous drug delivery of tofacitinib in human skin. Eur. J. Pharm. Biopharm. 159, 1–10. https://doi.org/10.1016/j.ejpb.2020.12.008.

Hernández, B., Pflüger, F., Kruglik, S.G., Ghomi, M., 2013. Characteristic Raman lines of phenylalanine analyzed by a multiconformational approach. J. Raman Spectrosc. 44, 827–833. https://doi.org/10.1002/jrs.4290.

Hong, H., Wang, Y., 2007. Derivatization with Girard reagent T combined with LC-MS/MS for the sensitive detection of 5-formyl-2′-deoxyuridine in cellular DNA. Anal Chem 79, 322–326. 10.1021/ac061465w.

John Wiley & Sons, Inc. SpectraBase; SpectraBase Compound ID=4KwNtDajJqj SpectraBase Spectrum ID=GhWXEmhuBn8 https://spectrabase.com/spectrum/GhWXEmhuBn8 (accessed 19/1/2023). [WWW Document], n.d.

John Wiley & Sons, Inc. SpectraBase; https://spectrabase.com/ad?a=SPECTRUM_1sk1IH8Yu2l&r=https://spectrabase.com/spectrum/1sk1IH8Yu2l (accessed 19/1/2023). [WWW Document], n.d.

Kampf, G., 2018. Benzalkonium Chloride. In: Antiseptic Stewardship. Springer International Publishing, pp. 259–370. https://doi.org/10.1007/978-3-319-98785-9_10.

Kwak, S., Brief, E., Langlais, D., Kitson, N., Lafleur, M., Thewalt, J., 2012. Ethanol perturbs lipid organization in models of stratum corneum membranes: An investigation combining differential scanning calorimetry, infrared and 2H NMR spectroscopy. Biochim. Biophys. Acta Biomembr. 1818, 1410–1419. https://doi.org/10.1016/j.bbamem.2012.02.013.

Lachenmeier, D.W., 2008. Safety evaluation of topical applications of ethanol on the skin and inside the oral cavity. J. Occup. Med. Toxicol. https://doi.org/10.1186/1745-6673-3-26.

Lau, W.M., Ng, K.W., 2017. Finite and infinite dosing. In: Percutaneous Penetration Enhancers Drug Penetration Into/Through the Skin: Methodology and General Considerations. Springer, Berlin Heidelberg, pp. 35–44. https://doi.org/10.1007/978-3-662-53270-6_3.

Leyden, J.L., Kligman, A.M., 1972. Treatment of alopecia areata with steroid solution. Arch. Dermatol. Arch. Dermatol. 106, 924.

Mcdonnell, G., Russell, A.D., Operations, L., Louis, S., 1999. Antiseptics and Disinfectants: Activity, Action, and Resistance, CLINICAL MICROBIOLOGY REVIEWS.

Meng, Y., Cheng, X., Wang, T., Hang, W., Li, X., Nie, W., Liu, R., Lin, Z., Hang, L., Yin, Z., Zhang, B., Yan, X., 2020. Micro-Lensed Fiber Laser Desorption Mass Spectrometry Imaging Reveals Subcellular Distribution of Drugs within Single Cells. Angewandte Chemie - International Edition 59, 17864–17871. https://doi.org/10.1002/anie.202002151.

Pena, A.M., Chen, X., Pence, I.J., Bornschlögl, T., Jeong, S., Grégoire, S., Luengo, G.S., Hallegot, P., Obeidy, P., Feizpour, A., Chan, K.F., Evans, C.L., 2020. Imaging and quantifying drug delivery in skin – Part 2: Fluorescence andvibrational spectroscopic imaging methods. Adv. Drug Deliv. Rev. https://doi.org/10.1016/j.addr.2020.03.003.

Pena-Rodríguez, E., Lajarin-Reinares, M., Mata-Ventosa, A., Pérez-Torras, S., Fernández-Campos, F., 2021. Dexamethasone-loaded lipomers: Development, characterization, and skin biodistribution studies. Pharmaceutics 13. https://doi.org/10.3390/pharmaceutics13040533.

Perry, W.J., Patterson, N.H., Prentice, B.M., Neumann, E.K., Caprioli, R.M., Spraggins, J. M., 2020. Uncovering matrix effects on lipid analyses in MALDI imaging mass spectrometry experiments. J. Mass Spectrom. 55 https://doi.org/10.1002/jms.4491.

Raj, S., Jose, S., Sumod, U.S., Sabitha, M., 2012. Nanotechnology in cosmetics: Opportunities and challenges. J. Pharm. Bioallied Sci. https://doi.org/10.4103/0975-7406.99016.

Ryabchykov, O., Popp, J., Bocklitz, T., 2018. Fusion of MALDI spectrometric imaging and Raman spectroscopic data for the analysis of biological samples. Front. Chem. 6 https://doi.org/10.3389/fchem.2018.00257.

Rzagalinski, I., Volmer, D.A., 2017. Quantification of low molecular weight compounds by MALDI imaging mass spectrometry – A tutorial review. Biochim. Biophys. Acta Proteins Proteom. https://doi.org/10.1016/j.bbapap.2016.12.011.

Saraiya, N. v., Goldstein, D.A., 2011. Dexamethasone for ocular inflammation. Expert Opin. Pharmacother. 12, 1127–1131. 10.1517/14656566.2011.571209.

Signor, L., Varesio, E., Staack, R.F., Starke, V., Richter, W.F., Hopfgartner, G., 2007. Analysis of erlotinih and its metabolites in rat tissue sections by MALDI quadrupole time-of-flight mass spectrometry. J. Mass Spectrom. 42, 900–909. https://doi.org/10.1002/jms.1225.

Silbey, R.J., 1995. Principles of Nonlinear Optical Spectroscopy. World Scientific.

Takeo, E., Sugiura, Y., Uemura, T., Nishimoto, K., Yasuda, M., Sugiyama, E., Ohtsuki, S., Higashi, T., Nishikawa, T., Suematsu, M., Fukusaki, E., Shimma, S., 2019. Tandem Mass Spectrometry Imaging Reveals Distinct Accumulation Patterns of Steroid Structural Isomers in Human Adrenal Glands. Anal. Chem. 91, 8918–8925. https://doi.org/10.1021/acs.analchem.9b00619.

Wang, S.S., Wang, Y.J., Zhang, J., Sun, T.Q., Guo, Y.L., 2019. Derivatization strategy for simultaneous molecular imaging of phospholipids and low-abundance free fatty acids in thyroid cancer tissue sections. Anal. Chem. 91, 4070–4076. https://doi.org/10.1021/acs.analchem.8b05680.

Wu, Q., Comi, T.J., Li, B., Rubakhin, S.S., Sweedler, J. v., 2016. On-Tissue Derivatization via Electrospray Deposition for Matrix-Assisted Laser Desorption/Ionization Mass Spectrometry Imaging of Endogenous Fatty Acids in Rat Brain Tissues. Anal. Chem. 88, 5988–5995. 10.1021/acs.analchem.6b01021.

Yamamoto, K., Klossek, A., Flesch, R., Rancan, F., Weigand, M., Bykova, I., Bechtel, M., Ahlberg, S., Vogt, A., Blume-Peytavi, U., Schrade, P., Bachmann, S., Hedtrich, S., Schäfer-Korting, M., Rühl, E., 2017. Influence of the skin barrier on the penetration of topically-applied dexamethasone probed by soft X-ray spectromicroscopy. Eur. J. Pharm. Biopharm. 118, 30–37. https://doi.org/10.1016/j.ejpb.2016.12.005.

Zhang, H., Shi, X., Vu, N.Q., Li, G., Li, Z., Shi, Y., Li, M., Wang, B., Welham, N. v., Patankar, M.S., Weisman, P., Li, L., 2020. On-Tissue Derivatization with Girard's Reagent P Enhances N-Glycan Signals for Formalin-Fixed Paraffin-Embedded Tissue Sections in MALDI Mass Spectrometry Imaging. Anal. Chem. 92, 13361–13368. 10.1021/acs.analchem.0c02704.